Formation Flying and Change Detection for the UNSW Canberra Space 'M2' Low Earth Orbit Formation Flying CubeSat Mission

Melrose Brown[1]
[1]UNSW Canberra Space, Canberra, Australia
Russell Boyce[1], **Andrew Lambert** [1], **Edwin G. W. Peters** [1], **Steve Gehly** [1], **Samuel Boland** [1], **Ryan Jeffreson** [1], **Anthony Kremor** [1], **Timothy Bateman** [1], **Chris Capon** [1], **Brenton Smith** [1], **George Bowden** [1], **Lauren Glina** [1], **Lily Qiao** [1], **Sudantha Balage** [1], **Komal Gupta** [1], [1], **Rizka Purwanto** [1], **Travis Bessell** [2], **Tom Reddell** [3], **James Bennett** [4], **Michael Lachut** [4], **Tim McLaughlin** [5],
[1]UNSW Canberra Space, [2]Clearbox Systems,[3]LeoLabs,[4]EOS Space Systems, [5]Pine Park Engineering Corp

ABSTRACT

The University of New South Wales, Canberra (UNSW Canberra) embarked on an ambitious CubeSatellite research, development, and education program in 2017 through funding provided by the Royal Australian Air Force (RAAF). The program consisted of M1 (Mission 1), M2 Pathfinder, and concludes with the formation flying mission M2. M2 is the final mission comprising two 6U CubeSatellites flying in formation using differential aerodynamic drag control. The M2 satellites were launched in a conjoined 12U form factor on RocketLab's 'They Go Up So Fast' launch in March 2021. On 10th September 2021 the spacecraft divided into two 6U CubeSats (M2-A and M2-B) under the action of a small spring force in their near-circular 550km, 45-degree inclination orbit. The formation is controlled by varying the spacecrafts' attitude, which creates a large variation in the aerodynamic drag force due to the change in the cross-sectional area from the large, double-deployable, solar arrays located on the zenith face of the spacecraft.

This paper presents the outcomes of the Formation Flying and Change Detection primary mission objectives for the mission. The results are generated by collecting and analysing optical and RF (Radio Frequency) space domain awareness sensor data from the ground and validating them against GPS (Global Positioning System) and attitude data downlinked from the spacecraft. The outcomes of the broader mission objectives, which include increasing the Technology Readiness Level for a suite of intelligent on-board optical and RF sensor technologies, will be presented in subsequent publications.

The results presented here comprise two major campaigns: 1.) The spacecraft separation campaign when the original 12U form factor deployed following launch split in half to form the M2-A and M2-B satellites, and 2) the demonstration of active formation control of the spacecraft via differential aerodynamic drag.

M2-A and M2-B underwent several major configuration changes during the spacecraft separation campaign. The results from ground-based sensors detecting the 12U spacecraft separating into two distinct (6U) objects are presented. The effect of the double-deployable solar arrays deployment on the relative orbital motion of the M2-A and M2-B spacecraft is illustrated and compared to data from optical and RF ground-based measurements taken during this window. The formation control campaign involved actively controlling the spacecraft via differential aerodynamic drag in order to significantly alter the separation distance. The mission demonstrated the capability to switch the leading spacecraft's position between M2-A and M2-B and to actively control separation distance ranging from 130km down to 1km. Formation control is achieved via open-loop, pre-scheduled, commands issued from the UNSW Canberra Space ground station. A two-stage modelling and simulation process is used to derive the scheduled attitude states. Firstly, a batch least squares orbit determination algorithm is applied to GPS data from a steady-state differential drag actuation period (where one spacecraft is in maximum drag and the other in its minimum drag attitude configuration). The batch least squares orbit determination is conducted out using the NASA General Mission Analysis Tool (GMAT), resulting in precise state estimates for each spacecraft and drag coefficient (C_d) estimates for both the maximum and minimum drag configurations. Predictions of trajectory for various attitude profiles can be produced by tailoring the

spacecraft's drag coefficients between the maximum and minimum values generated by the batch least squares state estimation process.

Ground-based optical and RF space domain awareness (SDA) sensor measurements collected during the manoeuvre campaign are compared to the spacecraft's GPS and attitude telemetry data. The SDA sensors are actively seeking to detect changes in the separation distance between the spacecraft. Initial results from an investigation into whether changes observed in photometric light curve signatures can signal the commencement of a differential drag manoeuvre are presented.

1. INTRODUCTION

UNSW Canberra's RAAF-funded 'M' mission program comprise 4 satellites launched over 3 missions[1]:

- M1 (mission 1) - a 3U form factor CubeSat for radio frequency (RF) maritime surveillance through collection of AIS and ADS-B beacons via software defined radios. Launched in 2018
- M2 Pathfinder - a 3U form factor CubeSat that reduces risk for M2 to demonstrate successful operation of key satellite bus technologies. Launched in 2020
- M2 - 2x6U formation flying CubeSats. Launched in 2021

M2 is the final mission of the series and was launched on 22nd March at 22:30UTC as a secondary payload onboard the Rocket Lab "They Go Up So Fast" Electron launch. The payloads integrated into M2 significantly advanced Australian small satellite technology within the frame of technology demonstration and TRL raising for maritime surveillance applications. The payloads onboard include 4 optical sensors (3m ground resolution main optical telescope, an in-house star tracker, neuromorphic events-based sensor, and a low fidelity 'selfie-cam' for inspection of the spacecraft bus); FPGA-based software defined radios for beacons detection from ships and aircraft; GPU processors for on-orbit artificial intelligence demonstration; and an inter-satellite laser link to support a world-fist "ionospheric aerodynamics" experiment.

M2 has several primary mission objectives that track the development and commissioning of the individual payload modules to fulfil the maritime surveillance, space domain awareness, and on-orbit artificial intelligence themes for the mission plan. We report here on the completion of the 'Change Detection' and 'Propulsion-Free Formation Flying' primary mission objectives that are central to the space domain awareness research theme. The change detection primary mission objective (PMO) centres on utilising optical, passive RF, and radar ground sensors to capture major changes to the spacecraft configuration from the ground. Telemetry from the spacecraft provides position, velocity, and attitude knowledge as a truth source to validate the conclusions derived from the ground-based sensors. The propulsion free formation flying PMO explores and demonstrates how changes to the spacecraft attitude can be exploited to tightly control the along track separation distance between spacecraft in Low Earth Orbit under the action of differential aerodynamic drag. The close proximity formation control experiments provide a challenging real-world target to support the change detection PMO.

The most prominent behaviours suitable for change detection analysis will occur during:

- Spacecraft separation - when the spacecraft splits in half to form 2x6U CubeSats
- Deployment of large solar arrays
- Stabilisation of the formation post separation via atmospheric drag
- Close proximity operations
- Changes to the spin and attitude stability of the spacecraft, from either operator commanded spins or spacecraft anomalies

The primary venue selected for performing the change detection and propulsion free formation flying experiments has been the Sprint Advanced Concept Training (SACT) space domain awareness experimentation cells [2]. The

Commercial SACTs are an international space operations experiment venue that run three times a year. SACTs are sponsored by the US Joint Task Force Space Defense (JTF-SD) and Department of Commerce (DOC) to exercise a wide variety of space domain awareness (SDA) vignettes centred on specific desired learning objectives (DLO) that cover a broad range of modern on-orbit space domain awareness scenarios. The DLOs include high-rate revisit sensor collection, conjunction assessment, application of space-based technologies, satellite anomaly detection, launch processing, manoeuvre detection, and many others.

SACT events aim to advance the state-of-the-art in space "Protect and Defend" missions, Safety of Flight, and Space Traffic Coordination (STC) through international collaboration of commercial, academic, US civil, and allied government agencies. SACTs are conducted from multiple geographic locations but are consolidated onto a virtual ops floor, thus enabling 24/7 operations by transitioning command and control between Americas, Pacific, and Meridian cells throughout the experiment. Common centralised control centres for SACT have included Sydney, Canberra, and Adelaide Australia; Colombelles, France; Colorado Springs, United States. Several nations participate in the event series including United Kingdom, Canada, Japan, France, Spain, Australia, India, South Korea, Netherlands, Poland, Italy, and others.

2. METHODS

2.1 Propulsion-Free Low Earth Orbit Formation Flying

Differential aerodynamic drag has been proposed as a propulsion free method for formation control in several previous works. Theoretical treatment supported by modelling and simulation have traditionally focused on the development of control algorithms based on the Hill-Clohessy-Wiltshire equations or modifications to those equation sets such as the Schweighart and Sedwick dynamics model [3][4][5][6][7]. Underpinning many of these approaches is the ability for communication of real-time position and velocity updates between the spacecraft, accurate knowledge of the local atmospheric density that feed an autonomous control system onboard both spacecraft.

Real-world applications of differential aerodynamic drag control include constellation deployment and phasing, such as the Cyclone Global Navigation Satellite System (CYGNSS) [8], Planet Flock deployments [9], ORBCOMM constellation[10], the AeroCube-4 CubeSats [11] and the S-NET formation[12]. The majority of these missions are typified by a close initial grouping of satellites following deployment from the launch vehicle. The goal for constellation deployment is to use differential aerodynamic drag to evenly distribute the spacecraft around the orbit plane. Efforts to utilise differential aerodynamic control for close proximity satellite formation control - where the spacecraft are controlled to operate 1-2km from each other - are rare. The JC2Sat mission [13] proposed demonstrating close formation control of around 100m via differential aerodynamic drag, however no details on the launch or on-orbit results have been found and we assume that the mission never launched.

To our knowledge, M2 is the first mission to attempt close proximity operations using differential aerodynamic drag. During the M2 mission along track separation has been controlled from 130km to 1km. A critical enabler for this method is the approach adopted to split the spacecraft pair from the 12U to 2x6U CubeSats. Failure to cleanly separate the spacecraft would risk entangling critical antennas and damage primary mission payloads, however the ΔV at separation must be small enough that differential aerodynamic drag can arrest the initial separation and stop the spacecraft from continually drifting apart. The 12U pair were commanded to separate into the M2-A (47967) and M2-B (47973) satellites through aligning the spacecraft in the along track direction before activating a burn wire. A small ΔV was imparted to each of the spacecraft via three springs between the spacecraft that were carefully sized and tested to ensure constraints for clean separation and maximum drift rate were met. Figure 1(a) shows the 12U conjoined pair deploying solar panels and adopting a low/high drag differential spacecraft attitude that is used for formation control.

Another key technology underpinning the differential aerodynamic control strategy are the large, double-deployable, solar arrays, depicted in Fig. 1(b). Each 6U satellite has a mass of 10.35kg, orienting the -Y face into the velocity direction provides the maximum drag area of 0.293 m^2; the +X face provides the minimum drag area of 0.043 m^2. The reaction control wheel system provides 3-axis attitude control to point the spacecraft into its nominal high (+Z ram direction) and low (+X ram direction) attitudes, using coarse sun sensors, magnetometers, and earth horizon sensors for attitude determination. Along track control is achieved through changing the attitude of the spacecraft from high drag to low drag to affect the orbital decay rates of M2A and M2B from differential aerodynamic drag. The position and velocity are measured with a Skytraq Venus 838 GPS receiver, with a reported uncertainty of +/-1.24m in position by the manufacturer. GPS data is recorded at 1minute intervals. Downlink of the GPS data is commanded from

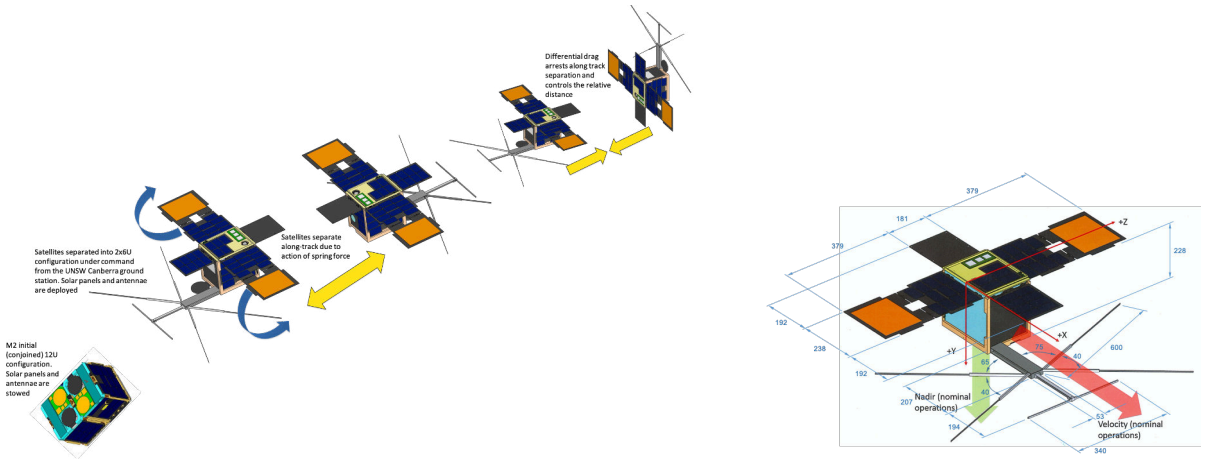

(a) Deployment and separation of the M2 satellite from a 12U CubeSat configuration into 2x6U

(b) Geometry of the fully deployed M2 spacecraft, measurements in mm

Fig. 1: M2 release/deployment and dimensions

the UNSW Canberra groundstation. The spacecraft pass over the UNSW Canberra ground station 6 times per day, however only 1 spacecraft is communicated with during a single pass. Priority can be given to one spacecraft over another, with nominal operations sharing the passes evenly between spacecraft.

Formation control is achieved through an open-loop approach that performs a batch least squares orbit determination on each spacecraft's downlinked GPS data to estimate position, velocity, and drag coefficient (C_d). The orbit determination provides accurate states for a subsequent high fidelity orbit propagation that models the effect of changing spacecraft attitude to generate the differential drag manoeuvre. The differential drag manoeuvre is modelled as a step change in drag coefficient. If both spacecraft are in the same pointing configuration (high drag, low drag, or tumbling), a scale factor is applied to the drag coefficient to approximate the planned manoeuvre. If the spacecraft are in opposite configurations (one in high drag, one in low drag) then the C_d estimates are swapped between the spacecraft to approximate the differential drag manoeuvre. GPS data is downlinked for each pass during the manoeuvre to successively refine the accuracy of the trajectory predictions for improved formation control accuracy.

Orbit propagations are performed using a 9th order Runge-Kutta integrator. The EGM-96 gravity model with 40th degree/order gravitational potential is applied; the Sun and Moon are included as 3rd body point masses. We use a spherical drag model with the MSIS-90 atmospheric density model, which is regularly updated with current and predicted F10.7, Kp, and ap space weather indices from the Center for Space Standards and Innovation (CSSI), hosted on the CelesTrak website. For past times, these are observed values from the Dominion Radio Astrophysical Observatory (F10.7) and GFZ Potsdam (Kp, ap). For future times, these are taken from the NOAA SWPC 45-day forecast. The weighted batch least squares measurement error model assumes a 10m noise sigma and zero bias. The noise sigma value was selected through trial and error to find the best balance between accuracy and robustness. The estimation is initialised with the first record in the GPS measurement file and C_d=1.5. The GPS measurement data from the spacecraft is filtered to include only high accuracy GPS data, defined here as when the system has a 3D fix and dilution of precision on position ≤ 2. Orbit determination is performed over time periods with constant high or low drag pointing, or a maximum of 3 days if the attitude has not altered. The exception to this approach is when the spacecraft automatically point to the UNSW Canberra ground station. Ground station pointing occurs 6 times per day and accounts for approximately 5% of the total orbit time per day. Periods of ground station pointing are therefore included in all of the orbit determination fits, as shown in Fig. 2(a)

The high-level approach for reducing the along track separation between the spacecraft is explained in the following steps and Fig. 2(b):

1. The chaser spacecraft is placed in a high drag configuration, the leader spacecraft maintains its default/nominal low drag attitude
    - The chaser drops in altitude relative to the leader, decreasing orbital period and thus reducing the along

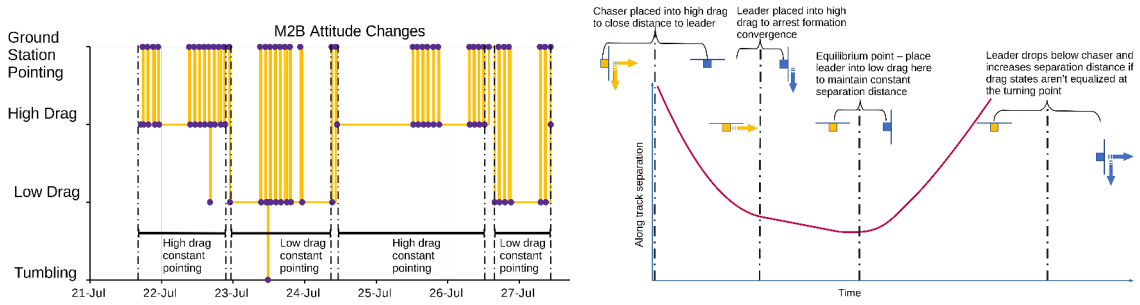

(a) Periods defined as continuous pointing for orbit determination

(b) Outline of differential aerodynamic control method

Fig. 2: M2 formation flying approach

track separation

2. After X days of high drag, the chaser is placed into a low drag configuration and coasts towards the leader (not shown in Fig. 2(b)).
    - The rate of decay between the chaser and leader is now constant, however the difference in altitude/semi-major axes maintains a convergence rate between the spacecraft
3. The leader is placed in high drag for X days to arrest the convergence and equalise the spacecraft altitudes/semi-major axes.

Several real-world challenges make the control method difficult: Dynamic changes to the Earth's atmospheric density manifest in substantial variation in C_d values over time due to deficiencies in the MSIS-90 empirical model and predicted space weather indices, which introduces uncertainty into the manoeuvre modelling process (discussed further in Subsection 2.1.1). Differences in C_d exist between the spacecraft when they are nominally in the same high or low drag state. The C_d differences arise from a combination of slight geometrical differences (due to e.g the deployment of a lens cap cover on M2B but not M2A) and errors/uncertainties in the attitude determination and control. Formation flying must also occur around the primary payload commissioning and operation activities, with the short breaks in high or low drag pointing highlighted in Fig. 2(a) to achieve the mission aims contributing to some uncertainty in the state estimation process.

The most significant operational challenge involves phasing the scheduling of telemetry downlink and issuing manoeuvre commands. With the constraint that only 1 spacecraft can be communicated with per pass, and any manoeuvre/attitude change commands formulated and validated before the pass starts, the timing of the sequence highlighted in Fig. 2(b) with the GPS downlink and operational decision making is critical. Spacecraft anomalies that prevent GPS data from being collected or the spacecraft to unintentionally tumble disrupt the orbit determination and manoeuvre planning process, requiring off-nominal scenario planning to ensure that the spacecraft will remain in a safe state.

Figure 3 charts the change in along track separation between M2-A and M2-B derived from analysis of two-line element (TLE) history provided by the public space-track.org TLE catalogue. Key events for the change detection and formation flying primary mission objectives are identified in the figure. The spacecraft separation event presented an ideal opportunity for cooperative space surveillance activity and is described in more detail in Section 3.

The execution weeks for the 3 SACT events are highlighted in Fig. 3. The spacecraft have been intentionally manoeuvred together to provide challenging close proximity Low Earth Orbit targets for the SDA sensor teams participating. The original plan for SACT 22-1 (November 15th-19th 2021) was affected by a strong G3 solar storm on 4th November that resulted in a decision to abort the close approach attempt and instead cross M2A and M2B over (switch leader/chaser order) to eliminate the risk of the spacecraft performing an unintentional rendezvous. The spacecraft have crossed over an additional three times on 5th June, 25th July, and 3rd August 2022. The crossover event in June was performed to place M2-B as the leader, which is the preferred orientation. The cross-over event on 25th July resulted from a mild geomagnetic storm coinciding with a 24hr period of downtime with ground segment, requiring a change from intended close approach formation flying for SACT 22-3 to a cross-over manoeuvre during SACT on

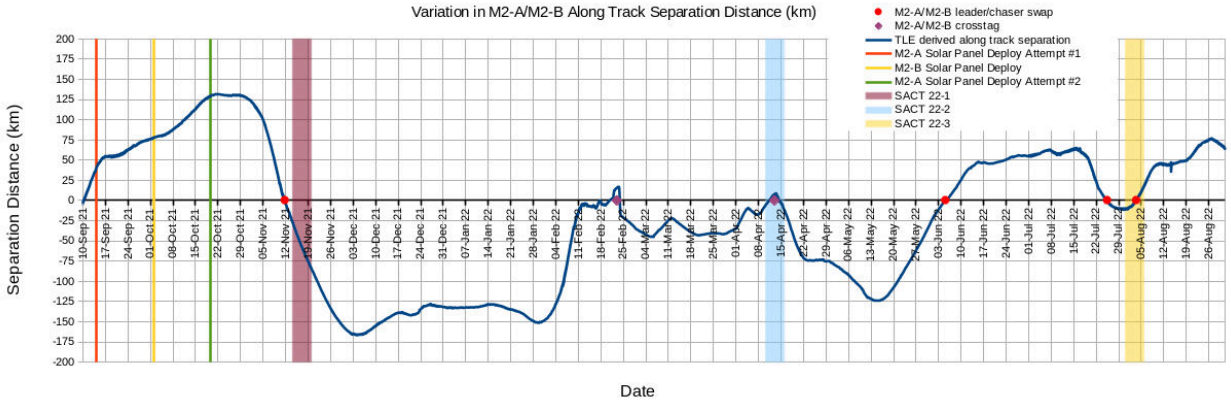

Fig. 3: Evolution of along track separation derived from Two Line Element history

3rd August. Two cross tag events are highlighted where the TLEs erroneously predict that spacecraft cross over. The cross tag events occurred during the formation flying practice attempt conducted on 23rd February in preparation for SACT 22-2, and on 13th April when M2-A and M2-B were successfully flown in close formation during the SACT 22-2 execution week.

2.1.1 Solar Weather Events and Impacts

Dynamic variation in the thermosphere represents a significant source of uncertainty in estimating drag forces acting on the M2 satellites. Satellite drag is a function of neutral density and also (less strongly) composition and temperature; quantities which vary significantly both spatially and temporally in LEO. The impact of geomagnetic storms due to coronal mass ejections (CMEs) and corotating interaction regions (CIRs) on these quantities can be large and is difficult to predict in advance. The MSIS-90 empirical model used here incorporates limited climatolgical data at high geomagnetic activities and therefore does not capture spatial and temporal storm-time variations very accurately [14]. Moreover, the orbit determination technique does not account for the effect of composition and temperature changes on C_d.

Geomagnetic activity impacted the formation flying mission on several occasions. Between 1st and 2nd November 2021 multiple CMEs were generated associated with solar active regions AR2887 and AR2891. The faster travelling, later CME overtook those ejected previously, producing compressed plasma with a complex magnetic field. When this combined CME reached Earth on 3rd November it resulted in a severe geomagnetic storm (peaking at G4). Multiple CMEs generated above solar active Estimates from the NRLMSISE-00 [15], Jachia Bowman 2008 [16], and DTM-2020 [17] empirical models are indicated in Figure 4(a) along with the corresponding space weather indices in Figure 4(b). The models show peak density enhancements of between 90% and 210%. The additional drag placed M2-B in a lower orbit than anticipated, preventing the close approach attempt planned for SACT 22-1.

Lower but non-negligible levels of geomagnetic activity were observed in the lead-up to SACT 22-2 and 22-3. On 8th April 2022 a CME left the sun, producing a brief, intense geomagnetic storm (peaking at G3) when the Earth was passing through its wake on 10th April. Minor geomagnetic storms (peaking at G1) occurred on 19th, 21st, and 23rd July. Space weather indices for these events are shown in Figure 4(c) and Figure 4(d) respectively.

2.2 Ground-based Space Domain Awareness Sensors for Trajectory Change Detection

A collaborative effort between radar, passive RF, and optical sensors was undertaken involving UNSW Canberra, Clearbox Systems, Electro Optics Systems (EOS), Pine Park Engineering (PPE), and LeoLabs Australia for the separation and three SACT events.

M2-A and M2-B both transmit on UHF at 449.538 MHz and utilise S-band for high rate downlink of data. For SACT 22-3, an experiment was conducted to enable M2-A to transmit constant tones at 2.42491 GHz and M2-B at 2.42511 GHz to generate simultaneous transmissions from both spacecraft with a 200kHz offset to enable unique identification and data association. UNSW Canberra is actively developing its combined optical and passive RF space

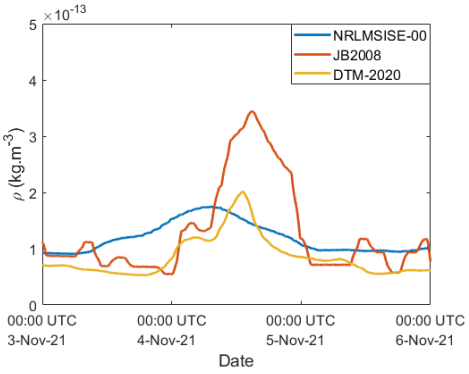

(a) Empirical model estimates for orbit mean thermosphere mass density during the November 2021 geomagnetic storm.

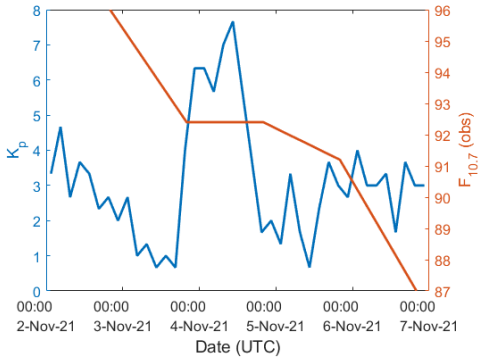

(b) Space weather indices during the November 2021 geomagnetic storm magnetic storm.

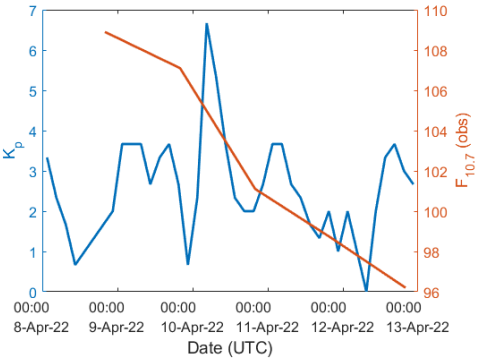

(c) Space weather indices during the April 2022 geomagnetic storm.

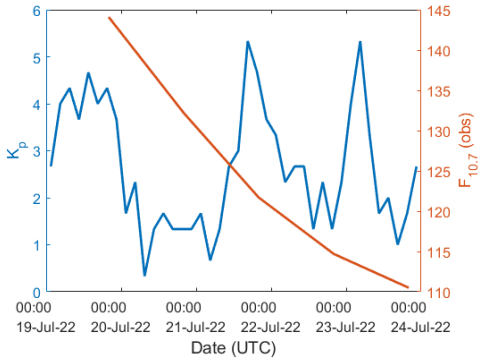

(d) Space weather indices during the July 2022 geomagnetic storms.

Fig. 4: Space weather indices for geomagnetic storms occurring near SACT events

domain awareness capability across UHF, S-band, and Ku-band. The M2 change detection experiments forms an important validation and development path for UNSW Canberra's contribution to the Cooperative Research Centre Project (CRC-P) "A sensor network for integrated Space Traffic Management for Australia", conducted in partnership with Clearbox Systems as the industry lead. UNSW Canberra seeks to combine passive RF and optical data for both orbit determination and characterisation of resident space objects, using a combination of 0.5m Raven Class telescopes from the Falcon Telescope Network[18] and the "VIPER" 2° field of view 0.36m Rowe-Ackerman-Schmidt Astrograph (RASA) for optical analysis. More information on the specifics of the sensors can be found in [19].

Clearbox Systems have supported the M2 mission from launch with their passive RF network 'SpaceAware' [20], which is under active development through the CRC-P research partnership with UNSW Canberra, Capricorn Space, and Bluerydge. The system will seek to detect actively transmitting satellites in the VHF, UHF, S, X and Ku bands, using a combination of omni-directional and directional antennas. Sites in Canberra and Adelaide were used in the work here to detect M2's UHF transmissions. Frequency estimation is performed on the collected data from the sensor network to generate range-rate measurements which can be used to refine orbit estimations. SNR observations are also generated in order to determine changes in SNR over time which could infer the stability of the satellites. The successful detection of transmissions from the spacecraft allow for indications that it's operating nominally, see Fig. 5, and any change in spacecraft transmissions can be captured as anomalous behaviour to prompt further investigation. For example, during SACT 22-1, it was detected that both spacecraft were simultaneously emitting weak beacon signals which was not expected behaviour as each satellite is expected to be RF quiet unless being communicated with and, as highlighted in 2.1, only one satellite is communicated with per pass over the ground station. Fig. 5(d) shows the beacon signals from the two spacecraft detected in the same pass following two different Doppler curves from the Adelaide sensor site.

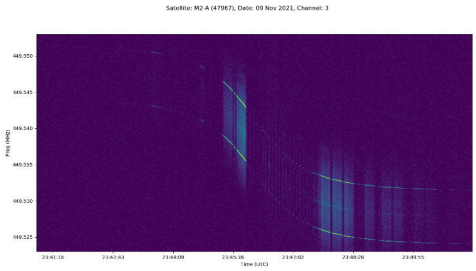

(a) RF power spectral density spectrum plot over time showing the emissions from the M2-A satellite.

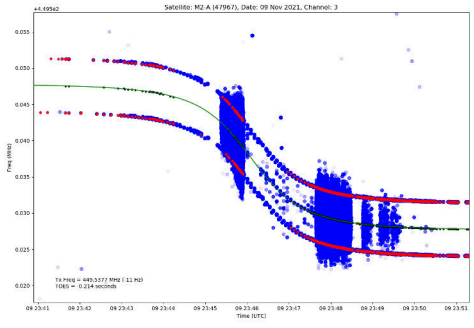

(b) Observed signal detected from the RF emissions that are above the noise floor. Blue dots are the peaks within the capture, red dots are the peaks that are associated to the spacecraft and the black dots are the estimates of the observed frequency over time. The green line represents the expected frequency observed based on the TLE.

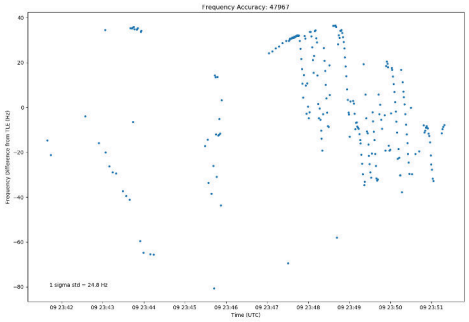

(c) Comparison of the observed frequency vs the expected frequency based on the TLE during the time period.

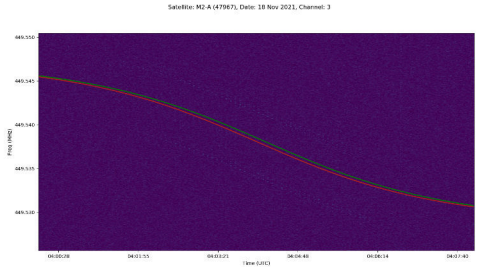

(d) Beacon signals captured from M2-A and M2-B during the same pass. The green line represents the Doppler curve based on the TLE of M2-A and the red line represents the Doppler curve based on the TLE of M2-B

Fig. 5: Clearbox Systems data capture and signal processing performed on a single pass of the M2-A satellite from the Adelaide sensor site

(a) 14s after separation (b) 20s after separation (c) 29s after separation

Fig. 6: Images from the separation event from M2-A looking at M2-B, commanded on 10th September 2021 at 04:55UTC

LeoLabs data was collected from a phased array network of 2 UHF and 5 S-band radars[21]. The radars act as a network, with automatic scheduling and prioritisation. Range and doppler are automatically measured, corrected and associated on site against expected object trajectories to form tracklets. Range and range rate are then fed into the LeoLabs cloud, and orbit determination is performed on the tracklets to produce or refine a state vector. State vector estimates are improved over successive passes using a Kalman filter. The resulting state vectors and raw measurements are then available for download via the LeoLabs API. UNSW Canberra researchers and students were provided user accounts to support early operations and participation in SACT events.

In support of the M2 satellite mission, EOS provided observations from its two tracking sites: Learmonth (22.221°S, 114.104°E) in Western Australia and Mt Stromlo (35.316°S, 149.010°E) in the Australian Capital Territory [22]. The network comprises 0.7m, 1m and 1.8m telescopes with both day and night tracking capabilities. Electro Optics Systems (EOS) have contributed photometric light curves, angles measurements, and state estimates derived from their optical data.

Pine Park Engineering (PPE) provided data from their two RASA-8 Astrograph LEO tracking Telescopes, located at the Pine Park Observatory outside of Colorado Springs [23]. PPE have a QHY-174M-GPS mounted in the front which yields a 1.6° x 1.0° FOV at F2.0.

3. SEPARATION

The 12U spacecraft split into 2x6U CubeSats on 10th October 2021 04:55UTC. The separation was the first major event following launch. The 12U conjoined pair were oriented in the along track direction, with M2-A receiving a positive along track thrust and M2-B a negative along track thrust from the spring release mechanism, resulting in M2-B having a shorter orbital period and thus leading M2-A (depicted as a positive along track separation distance in Fig. 3). Images from the on-board ‘selfie camera’ captured the separation event shortly after the burn wire command, with the images 14, 20, and 29s after the burn wire command shown in Fig. 6. The space domain awareness teams cooperated to monitor the spacecraft separation with the goal of identifying the deployment of M2-B from M2-A from ground-based sensors and searching for changes in characterisation data due to the solar panel deployment.

Clearbox Systems were the first to detect M2-B after separation via UHF passive RF, Fig. 7(a). Only one spacecraft transmits during a pass, however it was known ahead of time that the operation plan was to establish contact with M2-B first and the detection confirmed that the spacecraft was communicating. The first sensor to detect both objects was EOS performing a daytime collect with their 1.0m telescope at Learmonth, Fig. 7(b). The observations were collected at 2021-09-10T09:50:09Z (or 17:50:09 local time) and the two objects are both visible in the field of view (FoV), which is approximately 15 arc-minutes. The separation of the satellites during the pass was estimated by EOS to be approximately 1.15 km to 1.33 km.

UNSW Canberra captured M2-A and M2-B with the Colorado Mesa University node of the Falcon Telescope on 10th September 10:30UTC. Pine Park Engineering co-collected with their observatory for the same pass (Fig. 7(c)-7(e)). Both the Falcon and Pine Park sensors confirmed two objects present in the field of view. UNSW Canberra estimated an

along track separation between 1.3-1.4km from the images taken. Assigning M2-B as the leader required knowledge of the separation dynamics commanded by the spacecraft operators that wasn't available to Pine Park Engineering, however the photometric light curves in Fig. 7(d),7(e) both display elevated intensity mid-pass for the M2B satellite.

One of the primary mission objectives was to detect and characterise the delta-V imparted during the separation manoeuvre. One possible approach to estimate this ΔV using optical data would be to separately process angles-only measurements for each object following the manoeuvre using a batch least squares estimator, then compare the estimated state vectors at the separation epoch to compute the relative orbit states, and in particular, the relative velocity. However, given the quality and sparseness of measurements collected (a total of 24 observations were made in two short tracklets in the 30 hours following separation), the uncertainties in the estimated states would be too large to produce a meaningful estimate of the relative velocity at time of separation. Instead, the problem was reformulated in terms of relative orbit states and angles measurements. The optical data collected from the USAFA Falcon Telescope Network (FTN) site at Colorado Mesa University (CMU) was processed for photometric and relative orbit analysis. The dynamics were modelled with the linear Clohessy-Wiltshire (CW) equations. The relative intrack, radial, and crosstrack (RIC) components were fixed to zero at the time of separation and analysis performed to predict the impulsive separation velocity, assuming that the impulse occurs solely in the along track direction. As a linear model, the CW equations yield an analytic solution for spacecraft motion over time, as a function of 6 constants of integration, determined by the initial conditions. Measurement data is derived from images such as that shown in Fig. 7(c), taken approximately 5 ½ hours after the separation manoeuvre. A total of 24 images were collected over two optical passes depicting both spacecraft in frame at the same time. This allows computation of the relative angular separation in the sensor focal plane that can be mapped to the reference orbit for the spacecraft pair. The result from the optical measurements was an estimated separation velocity of 19.7mm/s, which agrees closely with the GPS derived estimate using the same approach (19.92mm/s) and the results from mechanical testing prior to launch that measured 18.9-19.3mm/s. The results from the analysis displaying the mean and 3σ boundaries are shown in Fig. 7(f).

The close proximity of the spacecraft and low relative velocities required a number of passes before M2B was sufficiently distinct for the data associator to assign M2B as a new object in the LeoLabs catalogue. The first state vector recorded for M2B became available on the platform on 11th September 02:00UTC.

Figure 8 presents the along track and radial distance between M2-A and M2-B processed from the GPS data. Data was collected at 1 minute intervals through the majority of the separation event, enabling a direct assessment of the spacecraft separation behaviour via a 9th order Hermite interpolation of the GPS files without the need to perform an orbit determination. The commanded separation at 04:55UTC has been confirmed through onboard sensors and the images shown in Fig. 6. The GPS uncertainty of +/-1.24m for both spacecraft plus the GPS data interpolation obscures a clear picture of the initial separation dynamics from the data, however by 05:16UTC the data clearly demonstrates that the spacecraft are drifting apart along track and have a clear radial offset. The along track separation estimates derived from early optical observations from EOS and UNSW Canberra are plotted on the figure.

3.1 M2B Panel Deployment

The next phase of the formation flying mission centred on arresting the spacecraft along track separation rate while simultaneously commissioning the 6U spacecraft pair. A passive differential aerodynamic drag approach was adopted, where the solar arrays on M2-A were deployed on 14th September 2021 at 02:50UTC and the panels on M2-B remained stowed to ensure a differential drag force could be maintained without the need for active pointing control on either spacecraft (Fig. 3). The goal for the formation flying PMO for this phase was to track the change in along track position and deploy M2-B solar arrays at the equilibrium point (Fig. 2(b)) to stabilise the formation and lock in a fixed along track separation distance. Access to the LeoLabs platform was critical during this phase, as high bandwidth S-band telemetry downlink was not yet commissioned for the spacecraft and downlinking sufficient GPS data within the time window available to provide an accurate orbit determination was uncertain. Figure 9 shows the refinement of estimated along track separation through successive LeoLabs state vector propagation. The data was used to determine a date for M2B solar panel deployment of 2nd October 2021 02:50UTC. Following successful deployment of the M2B solar arrays the LeoLabs platform highlighted that an unexpected large along track separation rate remained. The results were confirmed with an orbit determination performed with GPS data downlinked from the spacecraft. Further analysis revealed that the M2-A solar arrays had not fully deployed on 14th September. An additional burnwire command issued on 19th October 2021 14:26UTC rectified the issue and the spacecraft stabilised at approximately 131km along track separation on 20th October.

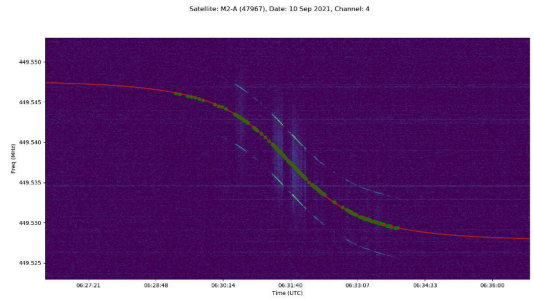

(a) Clearbox Systems: RF waterfall plot detecting the transmissions from M2-B following separation on 2021-09-10T06:27-06:36Z

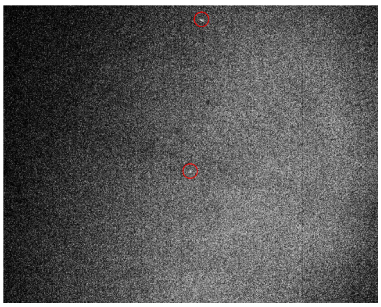

(b) EOS: M2-A and M2-B after separation at 2021-09-10T09:50:09Z, captured before sunset on a 1m telescope. Along track separation distance estimated at 1.15-1.33km

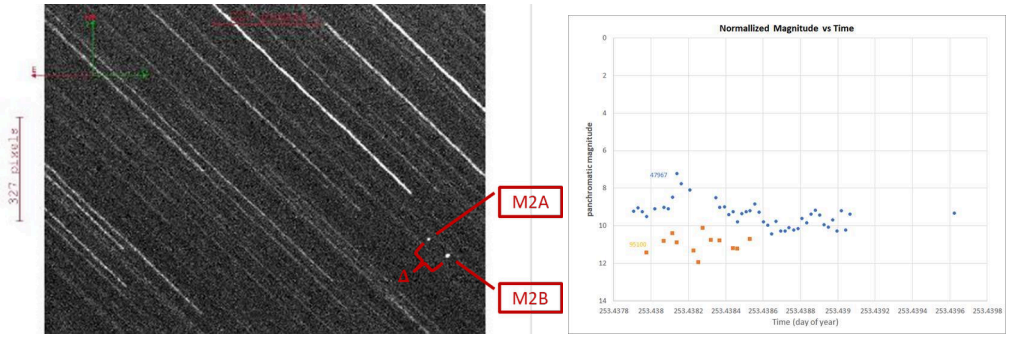

(c) UNSW: CMU-Falcon 2021-09-10 10:31:04 UTC, showing M2-A and M2-B separated by approximately 1.34km in the along track direction

(d) Pine Park Engineering: panchromatic visual magnitude of M2A and M2B from 2021-09-10T10:30Z

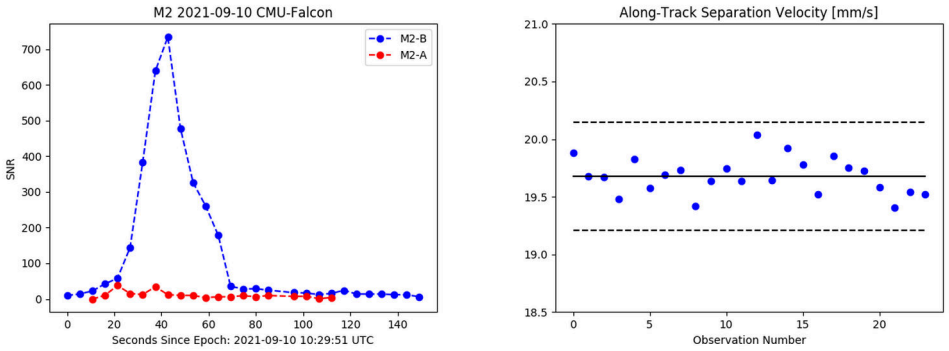

(e) UNSW: Light curve processed from 2021-09-10T10:30Z pass over the CMU Falcon node

(f) UNSW: Estimated ΔV spring force derived from CMU Falcon Node images

Fig. 7: Example optical and passive RF collects on M2-A and M2-B shortly after separation on 10th September 2021 from Adelaide, Learmonth, and Colorado

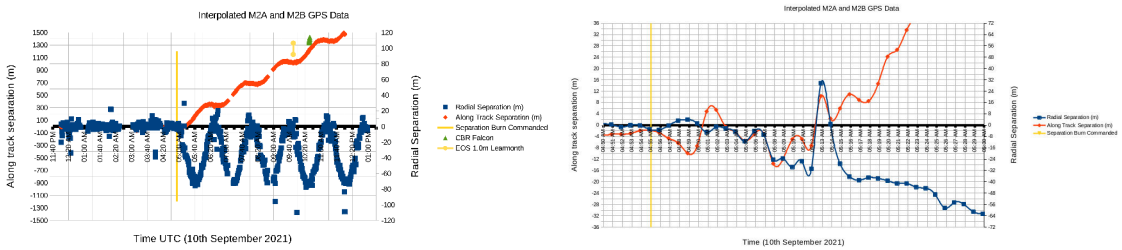

(a) 10th Sep 2021 00:00-10:20am (b) 10th Sep 2021 04:50-05:30am

Fig. 8: Relative Along Track and Radial Displacements derived from interpolated GPS data at 1minute intervals for 10th September 2021 confirm separation occurs at 04:55am

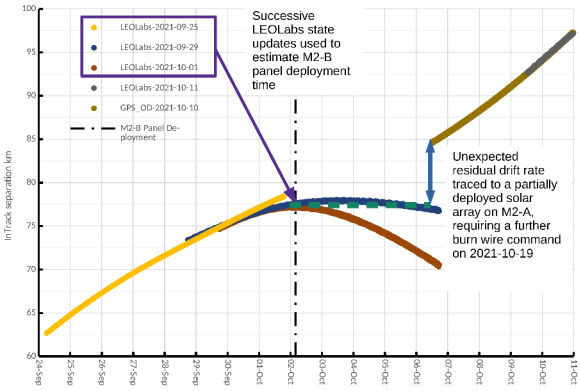

Fig. 9: Estimation of time for M2B solar panel deployment from LeoLabs state vectors

4. FORMATION FLYING AND CHANGE DETECTION ACTIVITIES DURING SPRINT ADVANCED CONCEPT TRAINING (SACT) 22-2

SACT 22-2 ran from 11th-15th April 2022. The week consists of two 24 hour vulnerability periods (VULs) where the global team of sensor providers actively track and analyse real-world and simulated on-orbit vignettes. The M2 goal for SACT 22-2 was to demonstrate that $\leq$5km formation flying could be achieved during the vulnerability periods for the event. The formation flying experiment therefore required execution of the formation flying manoeuvre within a tight window of time, placing additional complexities on the manoeuvre planning and operations. The challenge for the ground based sensors was to detect and characterise the close proximity formation flying experiment. In addition to the close proximity formation flying experiment, a spin stability characterisation experiment was added to the end of the close formation flying experiment, where M2-A would be commanded to tumble (rather than point). The aim was to test whether ground-based optical and RF senors could identify that M2-A was spinning and M2-B stable from photometric light curves and analysis of the signal to noise ratio in the passive RF signal.

A practice of the close proximity formation flying manoeuvre was performed from 30th January 2022 to 19th February. The spacecraft were converged from 150km separation distance to 2.5km on the 17th February. The practice proved out several operational and analysis approaches that were utilised in SACT 22-2. The primary difference between the practice and SACT 22-2 is that no specific date for achieving the close proximity formation flying was specified for the practice and no spin stability analysis was performed.

Figure 10 provides a high-level overview of the results from the SACT 22-2 formation flying experiment from the UNSW Canberra team. The change in along-track separation behaviour is highlighted in the main figure in the top right of Fig. 10. The TLE history in Fig. 3 shows that the spacecraft were 40km apart on 23rd March. The initial approach was aborted and the spacecraft retreated to 17km separation distance on 7th April to ensure the final close approach would occur during SACT 22-2. The figure plots the fitted GPS data (yellow) and the modelled manoeuvre

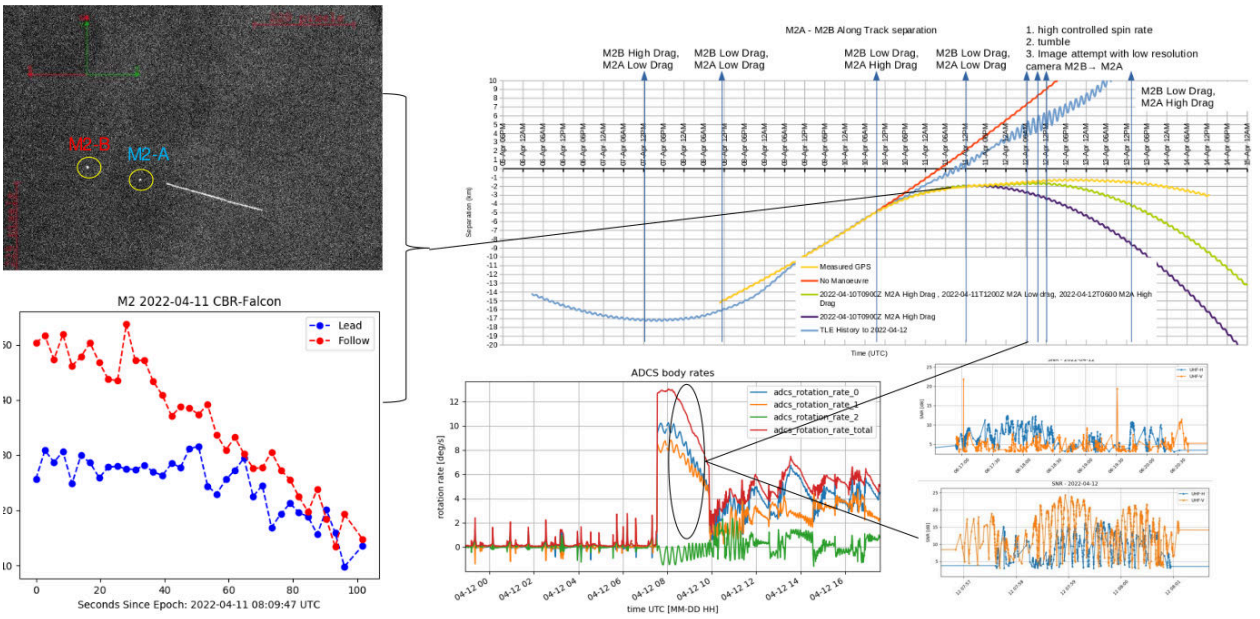

Fig. 10: Summary of the 2km close proximity formation manoeuvre and UNSW Canberra's ground-based optical and passive RF measurements for SACT 22-2 execution week

(green) used to plan the close approach. The manoeuvre was initiated with 24hrs of high drag for M2-B, beginning on 2022-04-7T10:26:27Z and placed into low drag on 2022-04-8T10:20:59Z for the remainder of the event. The high drag manoeuvre reduced M2B orbital energy and moved the spacecraft towards M2A. Without any further manoeuvres from M2A, M2B would have moved into the leader position on 11th April, indicated by the "No Manoeuvre" (red) curve in the figure. The TLE history follows the no manoeuvre line, resulting in a cross-tag of the spacecraft for a short period in the space-track catalogue.

M2-A performed a high drag attitude manoeuvre on 2022-04-10T08:27:38Z to begin stabilising the formation. The spacecraft switched to low drag on 2022-04-11T12:03:00Z when the spacecraft were predicted to reach near-equilibrium. M2-A was commanded to tumble on 2022-04-12T08:05:43Z and finally into high drag on 2022-04-13T06:12:44Z. A formation within -1.5km$\leq$-1.2km was maintained from 2022-04-12T09:00Z to 2022-04-13T09:00Z.

The weather prevented access with optical sensors for the majority of the live event, however the Canberra node of the Falcon Telescope Network captured a pass with both M2-A and M2-B in frame on 11th April 08:09UTC, on the evening prior to the first vulnerability live period. An example image and the dual light curve plots derived from the pass are shown on the left of Fig. 10. Both spacecraft are in ground station pointing mode through the pass, which is a dynamic and complex pointing manoeuvre for light curve analysis. The light curves demonstrate a higher intensity from M2-B during the pass, which requires further analysis through modelling and simulation to fully explore and explain. The dual lightcurve figure does highlight the potential for a comparative analysis of spin stability through imaging both spacecraft in the same frame.

In the scenario of close proximity formation flying, passive RF sensors have the ability to provide unique observations and avoid cross tagging based on the different emissions that are transmitted from the spacecraft to assist with orbit determination. This is typically a trivial task for passive RF sensors however M2-A and M2-B present a challenging scenario even for passive RF sensors as they operate on the same frequency and use the same modulation. Clearbox Systems attempted to determine if it's possible to detect subtle differences in the carrier frequency of the individual spacecraft based on the drift of the oscillators to assist with the problem of cross-tagging. Fig. 11 highlights some results of the centre frequency estimation where M2-A and M2-B satellites were successfully tagged based on the slight difference in the carrier frequency of their transmitters, which in this case, was approximately 80Hz difference. This technique enabled the two satellites to be identified and tagged successfully during short time periods (e.g. hours) as the change in drift is small but proved to be challenging to estimate over long time duration (e.g. days) where the individual drift of the oscillators is challenging to predict. Further research and analysis is required to determine if it's

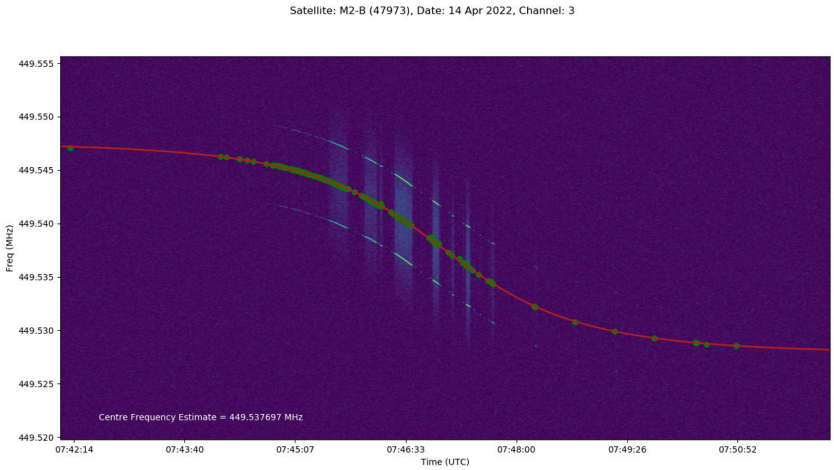

(a) RF spectrum waterfall plot from M2-B with an estimated carrier frequency of 449.537697MHz. The red line depicts the TLE and the green dots are the observed frequencies over time.

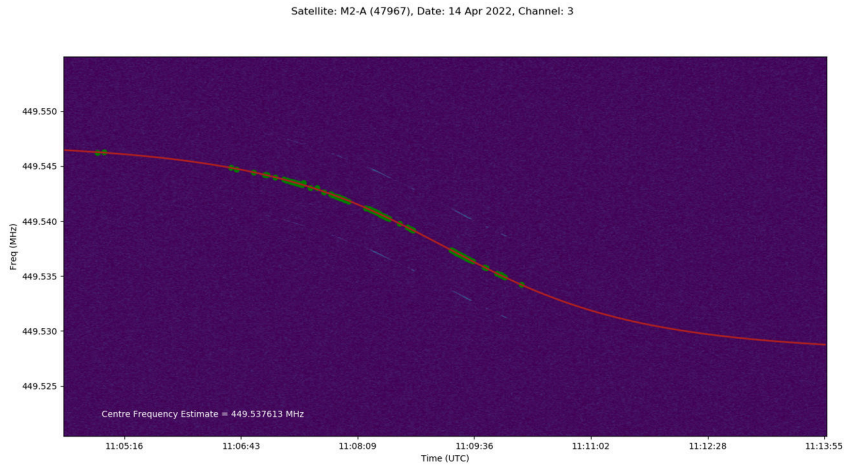

(b) RF spectrum waterfall plot from M2-A with an estimated carrier frequency of 449.537613MHz. The red line depicts the TLE and the green dots are the observed frequencies over time.

Fig. 11: Clearbox Systems RF waterfall spectrum plots detecting the transmissions from M2-A and M2-B along with the estimation of the carrier frequency during SACT 22-2

possible to maintain individual identification over long time periods.

The spin stability experiment on 12th April was performed principally with passive RF signal to noise ratio (SNR) from the UNSW Canberra passive RF sensors. Analysis of the SNR peaks and troughs generated by the null in the omni-directional UHF antenna pattern allow estimation of spin rates. Initial comparison with spin rates downlinked from the spacecraft indicate that good agreement with the 10°/second estimate from the SNR measurements. Pine Park Engineering obtained imagery that qualitatively confirmed the conclusion that M2-A was spinning optically, although cloud obscured the image at time.

5. FORMATION FLYING AND CHANGE DETECTION ACTIVITIES DURING SACT 22-3

The 22-3 SACT event took place during the week of 1st - 5th August 2022. The M2 mission implemented a constant S-band tone with a 200kHz offset between the spacecraft. The system was designed such that the S-band tones could be transmitted by both spacecraft simultaneously without disrupting operations. The approach provided an opportunity to combine optical and passive RF data sources to uniquely identify the leader and chaser spacecraft while operating

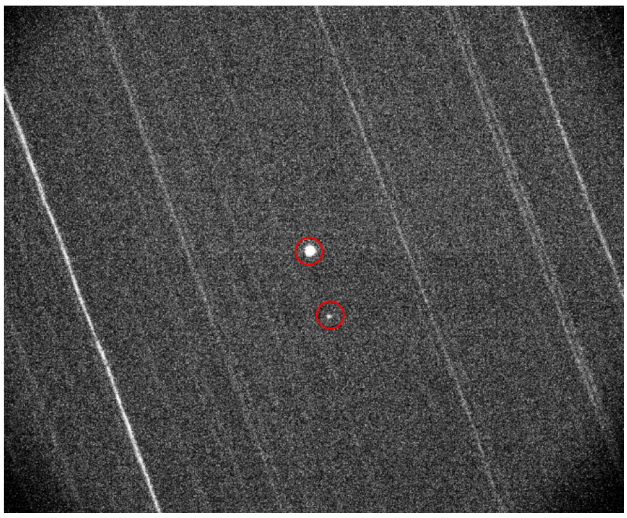

Fig. 12: EOS telescope image of M2-A (dimmer and off centre) and M2-B (centred and brighter) after passing by one another in-plane.

in close proximity. For this SACT, the spacecraft were intentionally crossed over on 3rd August, between the two vulnerability periods (Fig. 3). The change detection goals were to uniquely identify each spacecraft while in close proximity, determine whether the spacecraft crossed-over, and assess the spin stability of the spacecraft before and after the close proximity activity.

The results from the UNSW Canberra optical and passive RF campaign are reported in [19] a summarised here. The primary conclusions were:

- M2-B was confirmed to have crossed over with M2-A on 3rd August via the S-band passive RF sensors
- Optical lightcurves and RF signal to noise ratio characterisation indicated that M2-B was spinning prior to cross-over with M2-A. M2-B re-established spin stability after the cross-over event.
- Range measurements from unresolved radar measurements provide an opportunity to refine and enhance the analysis of optical telescope data to better estimate the along track separation between the spacecraft.

Clearbox Systems attempted to observe the S-band transmissions from the two spacecraft however the apertures used at the Adelaide and Canberra sites were too small to detect the faint transmissions. During SACT 22-3, Clearbox Systems successfully integrated the Capricorn Space sensor site into the 'SpaceAware' passive RF network which consists of two 5 metre S-band and X-band apertures. Further collections and analysis with this new sensor site will occur in future SACT events.

EOS provided additional optical surveillance of the formation close to the crossover time. The collections at 2022-08-03T09:27:13Z from Mt. Stromlo, Canberra, show the objects closer together with M2-B noticeably brighter than M2-A, as seen in Fig. 12. This provides supportive evidence that the attitude configuration differed for both objects relative to the ground station. These images were collected from a 0.7m telescope with a FoV of approximately 18 x 15 arc-minutes. The estimated separation during the EOS track in the case shown in Fig. 12 was approximately 760m which is easily resolvable in the image data collected. To analyse the behaviour of the formation flying of both M2-A and M2-B, the observation data collected was fitted using a batch-least squares orbit determination method to generate ephemeris data for the pair. The separation was then calculated and projected onto a RSW (radial, along-track, cross-track) body fixed coordinate frame using M2-A as the reference object.

In Fig. 13, it is evident that the separation is most pronounced in the along-track direction, where M2-A initially leads (negative along-track) but is eventually overtaken by M2-B in the orbital plane at approx. 2022-08-03T05:56:23Z. While M2-B's orbit is oscillating out-of-plane to M2-A's orbit by approximately ±30m, the average is near-zero indicating that they are virtually on the same orbital plane. The radial separation oscillates by approximately ±20m, but

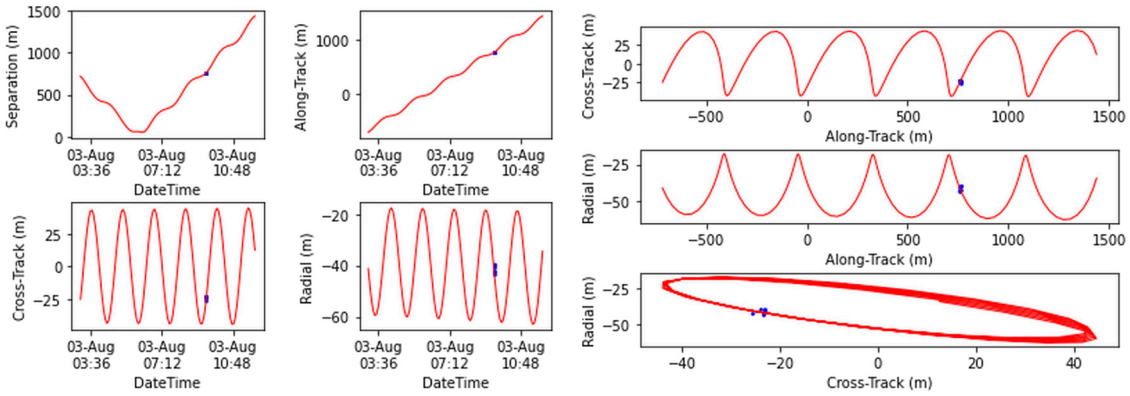

(a) Absolute separation and separation projected onto an RSW co-ordinate frame as function of time

(b) Absolute separation as function of time and separation projected onto an RSW coordinate frame looking from perspective of each plane of the RSW system

Fig. 13: Relative motion for M2A and M2B on 2022-08-03T from batch least squares orbit determination of EOS optical data. Red line – derived from ephemeris data. Blue dots – derived from observations

also has an estimated offset of -40m. This means M2-B has a slightly lower altitude – thus faster orbital velocity – explaining how it can overtake M2-A. The blue dots in Fig. 13 are derived from the observations and translated to the RSW system. They show good agreement with the red lines derived from fitted ephemeris data and are a visual verification of M2-B transit past M2-A.

6. CONCLUSIONS

The Propulsion Free Formation Flying and Change Detection primary mission objectives for the M2 formation flying CubeSat mission have been addressed in 3 campaigns, covering September 2021 to August 2022. The change detection mission objective has been made possible through a collaboration of sensors from UNSW Canberra, Clearbox Systems, Electro Optics Systems, LeoLabs, and Pine Park Engineering and lays a foundation for future multi-sensor data fusion experiments. The first campaign involved the observation and surveillance of the 12U M2 CubeSat splitting into the M2-A and M2-B 6U CubeSats. Optical sensors from EOS, UNSW Canberra/Falcon Telescope Network, and Pine Park Engineering detected both objects approximately 1km apart 5hours after the separation was commanded. Clearbox detected M2-B transmissions via passive RF shortly after separation and LeoLabs provided tracking data of the pair. Analysis of the tracklets obtained 5 hours after separation from the Colorado Mesa University node of the US Air Force Academy Falcon telescope network using the Clohessy-Wiltshire equations estimated a 19.7mm/s ΔV from the spring deployment mechanism. The results were validated against GPS data and correlated with the pre-launch tests during the assembly, integration, and verification phase of the mission.

Following separation, the formation was stabilised with the help of the LeoLabs API and platform, which provided successive state estimate updates to predict the time when the stabilisation manoeuvre should occur. The formation stabilised at 130km along track separation. Differential aerodynamic drag experiments were performed throughout 2022, centring on the Sprint Advanced Concept Training (SACT) events. The Propulsion Free Formation Flying primary mission objective was achieved when the spacecraft were flown within 1.2-1.5km of each other from 2022-04-12T09:00Z to 2022-04-13T09:00Z, providing the first on-orbit demonstration of differential aerodynamic drag to perform a close proximity formation flying manoeuvre. Data association activity from Clearbox Systems attempted to uniquely identify M2-A from M2-B through subtle differences from each spacecraft that nominally transmit on the same frequency. A novel spin stability characterisation approach developed by UNSW Canberra was performed that analysed the signal-to-noise ratio of the spacecraft transmissions that successfully detected the tumble introduced to M2-B on 12th April. Despite difficult weather conditions, optical analysis from Pine Park Engineering provided further evidence that the lead spacecraft was tumbling during this periods.

The last demonstration was in SACT 22-3 from 2nd-5th August 2022. The spacecraft were commanded to cross-over during between the SACT vulnerability windows. A combination of S-band passive RF and optical telescopes resulted

in a definitive measurement that M2-A and M2-B crossed over on 3rd August. Spin stability characterisation was performed with RF and photometric methods. EOS successfully performed an angles only orbit determination to analyse the relative orbital motion between the spacecraft over the close approach.

7. ACKNOWLEDGEMENTS

This work was funded by the Royal Australian Air Force, the Asian Office of Research and Development (AOARD), the Australian government round 9 Cooperative Research Centre Project (CRC-P) Scheme, and the University of New South Wales Canberra (UNSW Canberra).

Special thanks is given to Barbara Golf and Joseph Gerber for orchestrating the SACT and associated Dragon Army events; the Pacific Blue and White Cell leadership who have supported the M2 experiments within the SACT events; and all the people who have freely given their time to track or analyse the M2 mission.

[1] Melrose Brown, Brenton Smith, Christopher Capon, Rasit Abay, Manuel Cegarra Polo, Steve Gehly, George Bowden, Courtney Bright, Andrew Lambert, and Russell Boyce. Ssa experiments for the australian m2 formation flying cubesat mission. 2020.

[2] Joseph D Gerber, Yann Picard, Melrose Brown, Dr. Jason Held, Frederic Pelletier, and Timothy Fuller. Sprint advanced concept training (SACT), a renaissance in collaborative international space operations. In *Advanced Maui Optical and Space Surveillance Technologies Conference*, September 2020.

[3] Dave Guglielmo and Riccardo Bevilacqua. Propellant-less atmospheric differential drag leo spacecraft (paddles) mission. In *Proceedings of the 2014 SmallSat Conference*. Digital Commons Berkeley, CA, 2014.

[4] Christopher S Ruf, Clara Chew, Timothy Lang, Mary G Morris, Kyle Nave, Aaron Ridley, and Rajeswari Balasubramaniam. A new paradigm in earth environmental monitoring with the cygnss small satellite constellation. *Scientific reports*, 8(1):8782–13, 2018.

[5] David Pérez and Riccardo Bevilacqua. Lyapunov-based adaptive feedback for spacecraft planar relative maneuvering via differential drag. *Journal of Guidance, Control, and Dynamics*, 37(5):1678–1684, 2014.

[6] M Horsley, S Nikolaev, and A Pertica. Small satellite rendezvous using differential lift and drag. *Journal of Guidance, Control, and Dynamics*, 36(2):445–453, 2013.

[7] Constantin Traub, Francesco Romano, Tilman Binder, A Boxberger, GH Herdrich, S Fasoulas, PCE Roberts, Katharine Smith, Steve Edmondson, Sarah Haigh, et al. On the exploitation of differential aerodynamic lift and drag as a means to control satellite formation flight. *CEAS Space Journal*, 12(1):15–32, 2020.

[8] Charles D Bussy-virat, Aaron J Ridley, Abhay Masher, Kyle Nave, and Marissa Intelisano. Assessment of the Differential Drag Maneuver Operations on the CYGNSS Constellation. *IEEE Journal of Selected Topics in Applied Earth Observations and Remote Sensing*, 12(1):1–9, 2019.

[9] Cyrus Foster, James Mason, Vivek Vittaldev, Lawrence Leung, Vincent Beukelaers, Leon Stepan, and Rob Zimmerman. Constellation Phasing with Differential Drag on Planet Labs Satellites. *Journal of Spacecraft and Rockets*, 55(2):1–11, 2017.

[10] TD Maclay and Christopher Tuttle. Satellite stationkeeping of the orbcomm constellation via active control of atmospheric drag: operations, constraints, and performance (aas 05-152). *Advances in the Astronautical Sciences*, 120(1):763, 2005.

[11] Joseph Gangestad, Brian Hardy, and David Hinkley. Operations, orbit determination, and formation control of the aerocube-4 cubesats. 2013.

[12] Zizung Yoon, Walter Frese, and Enrico Stoll. In-orbit performance of the narrowband intersatellite mission s-net. In *2022 IEEE Space Hardware and Radio Conference (SHaRC)*, pages 1–4. IEEE, 2022.

[13] Keisuke Yoshihara, Marleen van Mierlo, Alfred Ng, B Shankar Kumar, Anton De Ruiter, Yutaka Komatsu, Hiroshi Horiguchi, and Hidekazu Hashimoto. Jc2sat-ff: an international collaboration nano-sat project—overview of the system analyses and design. In *Small Satellite Systems and Services (4S) Symposium, Rhodes, Greece*, 2008.

[14] JM Picone, AE Hedin, D Pj Drob, and AC Aikin. Nrlmsise-00 empirical model of the atmosphere: Statistical comparisons and scientific issues. *Journal of Geophysical Research: Space Physics*, 107(A12):SIA–15, 2002.

[15] JM Picone, AE Hedin, D Pj Drob, and AC Aikin. NRLMSISE-00 empirical model of the atmosphere: Statistical comparisons and scientific issues. *Journal of Geophysical Research: Space Physics*, 107(A12):SIA–15, 2002.

[16] Bruce Bowman, W Kent Tobiska, Frank Marcos, Cheryl Huang, Chin Lin, and William Burke. A new empirical thermospheric density model JB2008 using new solar and geomagnetic indices. In *AIAA/AAS astrodynamics specialist conference and exhibit*, page 6438, 2008.

[17] Sean Bruinsma. The DTM2020 models. In *43rd COSPAR Scientific Assembly. Held 28 January-4 February*, volume 43, page 813, 2021.

[18] Francis K. Chun, Roger D. Tippets, David M. Strong, Devin J. Della-Rose, Daniel E. Polsgrove, Kimberlee C. Gresham, Joshua A. Reid, Casey P. Christy, Mark Korbitz, Joel Gray, Stanton Gartin, David Coles, Ryan K. Haaland, Russ Walker, Jared Workman, John Mansur, Victoria Mansur, Terry Hancock, Julia D. Erdley, Thomas S. Taylor, Richard A. Peters, Christopher X. Palma, William Mandeville, Steven Bygren, Christian Randall, Kevin Schafer, Tim McLaughlin, José Luis Nilo Castellón, Amelia Cristina Ramirez Rivera, Hector Andres Cuevas Larenas, Andrew Lambert, Manuel Cegarra Polo, David Blair, Mark Gargano, Jan Devlin, Richard Tonello, Carsten Wiedemann, Christopher Kebschull, and Enrico Stoll. A new global array of optical telescopes: The falcon telescope network. *Publications of the Astronomical Society of the Pacific*, 130(991):095003, July 2018.

[19] Edwin Peters, Melrose Brown, Andrew Lambert, Lauren Glina, Timothy Bateman, Ed Kruzins, Rabbia Saleem, Travis Bessell, Tom Wnag, Tim Spitzer, Kriti Tripathi, Damian Huxtable, Michael Soire, Simon Zinsli, Thomas Powles, Isabella Federle, Mark Aragon, Adam Haskard, Mark Thompson, Warren Nielsen, and Russell Boyce. A sensor network for integrated space traffic management for australia. In *Advanced Maui Optical and Space Surveillance Technologies Conference*, September 2022.

[20] Mohd Noor Islam, Thomas Q. Wang, Samuel Wade, Travis Bessell, Tim Spitzer, and Jeremy Hallett. Doppler and angle of arrival estimation from digitally modulated satellite signals in passive rf space domain awareness. In *22nd Advanced Maui Optical and Space Surveillance Technologies Conference (AMOS 2021)*, pages 694–707, Maui, Hawaii, 2021. Maui Economic Development Board.

[21] James Rowland, Darren McKnight, Bonnie Prado Pino, Benedikt Reihs, and Matthew A Stevenson. A worldwide network of radars for space domain awareness in low earth orbit. 2021.

[22] C Smith, Ben Greene, Matt Bold, and Rod Drury. Development of a new ssa facility at learmonth australia. In *Proceedings of the Advanced Maui Optical and Space Surveillance Technologies Conference*, 2018.

[23] Tim McLaughlin and Roger L Mansfield. Observations of space object 2020 so using 8-inch f/2 schmidt astrograph. 2021.